A&A 530, A37 (2011)
DOI: 10.1051/0004-6361/201116820

Astronomy & Astrophysics

A stringent upper limit to SO_2 in the Martian atmosphere

T. Encrenaz[1], T. K. Greathouse[2], M. J. Richter[3], J. H. Lacy[4], T. Fouchet[1,5,6], B. Bézard[1], F. Lefèvre[5,7], F. Forget[5,8], and S. K. Atreya[9]

[1] LESIA, Observatoire de Paris, CNRS, 92195 Meudon, France
e-mail: therese.encrenaz@obspm.fr
[2] SwRI, Div. 15, San Antonio, TX 78228, USA
[3] Physics Department, University of California, Davis, CA 95616, USA
[4] Department of Astronomy, University of Texas at Austin, TX 78712-1083, USA
[5] Université Pierre et Marie Curie (UPMC), 75005 Paris, France
[6] Institut Universitaire de France, 75005 Paris, France
[7] UVSQ, CNRS/INSU, LATMOS/IPSL, Boite 102, 75005 Paris, France
[8] LMD/IPSL, UVSQ, CNRS/INSU, 75231 Paris, France
[9] Department of Atmospheric, Oceanic and Space Sciences, University of Michigan, Ann Arbor, MI 48109-2143, USA

Received 3 March 2011 / Accepted 22 March 2011

ABSTRACT

Surfur-bearing molecules have been found at the surface of Mars by the Viking lander, the Spirit and Opportunity rovers, and the OMEGA infrared spectrometer aboard Mars Express. However, no gaseous sulfur-bearing species have ever been detected in the Martian atmosphere. We search for SO_2 signatures in the thermal spectrum of Mars at 7.4 μm using the Texas Echelon Cross Echelle Spectrograph (TEXES) at the NASA Infrared Telescope Facility (IRTF). Data were obtained on Oct. 12, 2009 (Ls = 353°), in the 1350–1360 cm^{-1} range, with a spatial resolution of 1 arcsec (after convolution over three pixels along the N-S axis and two steps along the E-W axis) and a resolving power of 80 000. To improve the signal-to-noise ratio (S/N), we co-added the Martian spectrum around the positions of nine selected SO_2 transitions with a high S/N and no telluric contamination. From a mean spectrum, averaged over 35 pixels in the region of maximum continuum, we infer a 2σ upper limit of 0.3 ppb to the SO_2 mixing ratio, assuming that our instrumental errors are combined according to Gaussian statistics. Our upper limit is three times lower than the upper limit derived by Krasnopolsky (2005, Icarus, 178, 487), who used the same technique on previous TEXES data. In addition, we derive an upper limit of 2 ppb at each spatial pixel of the region observed by TEXES, which covers the longitude ranges 50 E–170 E for latitudes above 30 N, 100 E–170 E for latitudes between 0 and 30 N, and 110 E–170 E for latitudes between 15 S and 0. The non-detection of localized SO_2 sources in the observed area is consistent with a homogeneous distribution being expected around equinox for non-condensible species with a lifetime longer than the global mixing time. In view of the typically large SO_2/CH_4 ratio observed in terrestrial volcanoes, and assuming a comparable volcanic composition for Mars and the Earth, our result reaffirms that a volcanic origin is unlikely for any methane in the Martian atmosphere.

Key words. planets and satellites: atmospheres – infrared: planetary systems – planets and satellites: individual: Mars

1. Introduction

Sulfur-bearing molecules have been known to exist on the surface of Mars since the Viking era. The surface chemistry experiments of the Viking landers detected sulfates in the soil with abundances of 5 to 10 wt% (Toulmin et al. 1977). More recently, the Spirit and Opportunity rover experiments reported the detection of sulfates (in particular ferric sulfates and magnesium sulfates) at the Gusev and Meridiani sites (Squyres et al. 2004; Rieder et al. 2004; Johnson et al. 2007).

Attempts have also been made to search for sulfate signatures in the infrared spectrum of Mars. Roush et al. (1989) and Pollack et al. (1991) reported the detection of sulfate features in the 8–10 μm-region, which is consistent with the presence of 10 to 15 wt% of sulfates in the airborne dust. Christensen et al. (2004), using the Miniature Thermal Emission Spectrometer (Mini-TES) aboard the Opportunity rover, detected magnesium and calcium sulfates in outcrops at Meridiani Planum. Finally, using the OMEGA infrared imaging spectrometer aboard the Mars Express orbiter, Bibring et al. (2005) identified sulfates in many places on the Martian surface. In particular, Langevin et al. (2005) detected calcium-rich sulfates (gypsum), at high northern latitudes (240 E, 80 N), in a region corresponding to the dark longitudinal dunes of Olympia Planitia.

However, no sulfur-bearing gaseous molecule has ever been detected in the Martian atmosphere. This discovery would have major implications, as it would be the signature of ongoing outgassing activity. As shown by the high-resolution images of Mars Express (Neukum et al. 2004), the latest traces of volcanism on Mars should only be 2 million years old, so the possibility of a weak, present seepage being produced by some low-level volcanic or geothermal activity cannot be excluded.

After water vapor, carbon dioxide and sulfur dioxide are the most abundant gases emitted by terrestrial volcanoes. If comparable emission is found for Mars and the Earth, sulfur dioxide seems to provide the optimal means of searching for traces of present day volcanic activity on Mars. This outgassing could also be associated with methane, whose tentative detection has

been reported (Formisano et al. 2004; Mumma et al. 2009); in this case, the CH_4/SO_2 ratio could provide a constraint on the origin of the outgassing.

Several unsuccessful attempts have been made to detect SO_2 in the past, leading to a stringent limit of 1 ppb from thermal infrared spectroscopy (Krasnopolsky 2005), and another limit of 2 ppb from submillimeter heterodyne spectroscopy (Nakagawa et al. 2009). Because the photochemical lifetime of SO_2 is shorter than two years (Krasnopolsky 2005; Wong et al. 2003, 2005), a continuous search for SO_2 on a timescale of a few years is required.

In this article, we report on a search for SO_2 performed with the Texas Echelon Cross Echelle Spectrograph (TEXES) at the NASA Infrared Telescope Facility (IRTF). We took advantage of the imaging capabilities of TEXES to search for SO_2 over each spatial pixel of the disk. Our analysis leads to an SO_2 upper limit (2σ) of 2 ppb in each spatial pixel (which corresponds to a field of view of about 1000 km near the disk center), and a disk-averaged 2σ upper limit of 0.3 ppb, i.e. three times smaller than the value reported by Krasnopolsky (2005). Section 2 describes the observations. Section 3 presents the analysis and our results are discussed in Sect. 4.

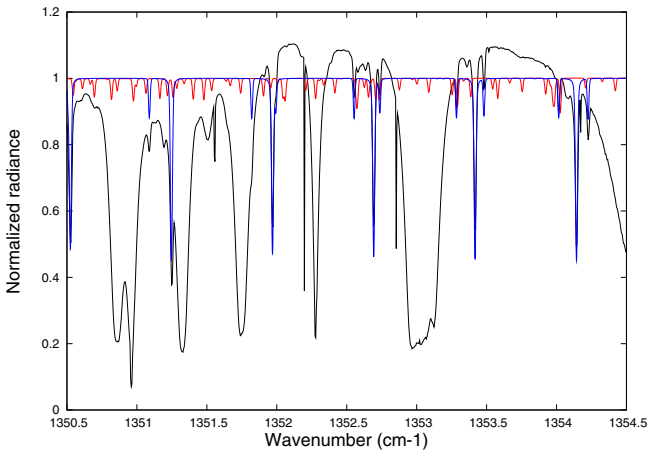

Fig. 1. The spectrum of Mars recorded by the TEXES instrument (black line), integrated over a region of 35 pixels centered on the maximum flux (longitude 140 E, latitude 30 N). The strong bands around 1350.9, 1351.35, 1351.75, 1352.25, and 1353.0 cm^{-1} are due to telluric absorption. Models: CO_2 (mixing ratio = 0.95, blue) and SO_2 (mixing ratio = 100 ppb, red).

2. Observations and data modeling

TEXES is an echelon cross-echelle spectrograph, which provides both high spatial and spectral resolutions in the 6–26 μm range (Lacy et al. 2002). Since 2001, we have mapped the Martian disk with the TEXES instrument at the IRTF, with the prime objective of detecting and mapping hydrogen peroxide (Encrenaz et al. 2004, 2008). In addition, we have been using weak transitions of HDO to monitor the water vapor simultaneously (Encrenaz et al. 2005, 2008, 2010). The observing run described in this paper was performed on October 11–15, 2009. A marginal detection of H_2O_2 was achieved, leading to a mean mixing ratio of 15 ppb over the disk (Encrenaz et al. 2011).

With a strength of 345 $cm^{-2}\,atm^{-1}$, the ν_3 band of sulfur dioxide is by far the strongest ro-vibrational band of this molecule. It exhibits a very large number of individual transitions with a maximum intensity in the 1350–1375 cm^{-1} range. We observed this entire spectral range over two different nights, but decided to concentrate on the 1350–1360 cm^{-1} range, since both the signal-to-noise ratio (S/N) and the atmospheric transmission there were better.

The 1350–1360 cm^{-1} range was observed on Oct. 12 between 15:00 UT and 19:00 UT. The diameter of Mars was 6 arcsec. The small apparent size of the disk limited our mapping capability. As in our previous runs, our spatial resolution was 1 arcsec, after convolution over three pixels along the N-S axis and two steps along the E-W axis. The observations took place slightly before northern vernal equinox (Ls = 353°). On Oct. 12 at 17:00 UT, the mean latitude and longitude of the disk center were 14.5 N and 140 E, respectively; the subsolar point was located at 3.0 S and 103 E. The terminator was situated on the evening side. The local hour at the center of the disk was 14:00. The radial velocity was –12.7 $km\,s^{-1}$, corresponding to a Doppler shift of +0.057 cm^{-1} at 1355 cm^{-1}. The spectral resolution was 0.017 cm^{-1} ($R = 8.0 \times 10^4$), and the spectral pixel size 0.0045 cm^{-1}. Velocities caused by the rotation of Mars are about 250 m/s at the east and west limbs, which corresponds to a Doppler shift of 0.0011 cm^{-1} at 1350 cm^{-1}, i.e. 0.25 times the size of the spectral pixel. Thus, the rotation effect can neither be detected with our observations nor influence our results.

The observing sequence was the same as for previous runs on Mars: the 1.1×8 $arcsec^2$ slit was oriented along the celestial N-S axis (the north polar axis of Mars was 349°CCW off the celestial north axis) and moved from west to east in 0.5 arcsec steps. Each map was acquired in about 10 min. The maps were co-added by superimposing the maximum flux measured in the continuum. The individual pixel size was 0.368 arcsec. To correct for possible defects associated with the pointing accuracy and the stability of the observations, our data were convolved over three pixels along the slit (N-S axis), and over two steps in the perpendicular direction (E-W axis). The resulting spectral resolution is 1 arcsec, as in the case of our previous TEXES runs. The data reduction and radiance calibration are described in Encrenaz et al. (2004, 2005).

Figure 1 shows a TEXES spectrum between 1350.45 and 1354.45 cm^{-1}, averaged over 35 pixels in the region of the disk where the continuum is maximum (see below, Fig. 2). The strong absorption bands around 1350.9, 1351.35, 1351.75, 1352.25, and 1353.0 cm^{-1} are due to terrestrial absorptions by CH_4 and H_2O. We also show in Fig. 1 a model of the Martian CO_2 isotopic (628) lines and a synthetic spectrum of SO_2 corresponding to a mixing ratio of 100 ppb. To model the synthetic spectrum of Mars, we used the CO_2 and SO_2 spectroscopic data from the GEISA data bank (Jaquinet-Husson et al. 2008). We adopted as an initial guess the temperature atmospheric parameters extracted from the Mars Climate Database of the Laboratoire de Meteorologie Dynamique (Forget et al. 2009) and adjusted these parameters to fit the CO_2 lines. We used a mean effective surface temperature of 240 K, a mean surface pressure of 5.8 mbars, and an airmass of 1.05. The atmospheric temperature is 225 K for $z = 0$ km, 198 K for $z = 10$ km, and 171 K at $z = 20$ km.

Figure 2 shows the TEXES map of the continuum radiance, averaged over two spectral pixels on each side of the CO_2 line at 1354.015 cm^{-1}. The point of maximum flux is located along the central meridian at a latitude of about 30 N. The spectrum shown in Fig. 1 is integrated over 53 spatial pixels centered on this position of maximum radiance. Figure 3 shows the fit between the integrated spectrum (Fig. 1) and our model in the weak CO_2 transition at 1354.015 cm^{-1}. Figure 4 shows the map of the line depth of this transition. This line depth is a function of

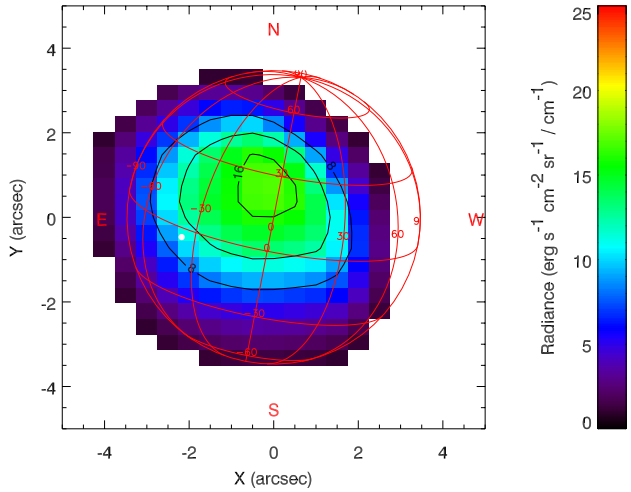

Fig. 2. The TEXES map of the continuum radiance averaged over two frequencies on each side of the 1354.015 cm^{-1} CO_2 line. The spatial resolution, after convolution, is 1 arcsec in each dimension. The size of the Martian disk is 6 arcsec. The longitude of the central meridian is 140 E. The white dot corresponds to the sub-solar point. Units are in arcsec in the celestial coordinates.

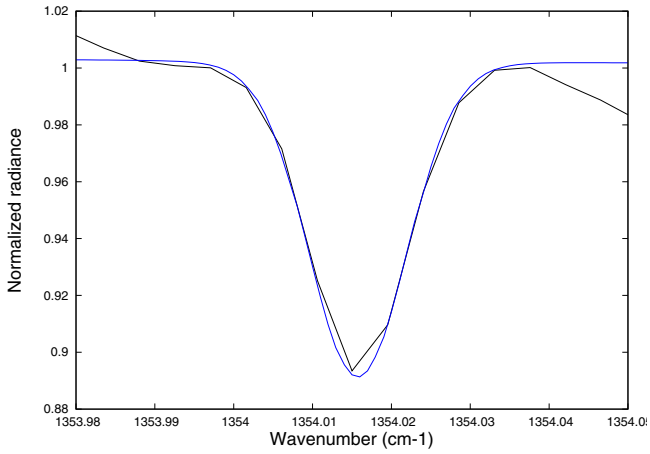

Fig. 3. The TEXES averaged spectrum around the 1354.015 cm^{-1} CO_2 line (black line), normalized to its continuum, compared with the synthetic model (blue line).

different factors: temperature contrast between the atmosphere and the surface, airmass, and topography. Figure 4 shows that the CO_2 line depth is larger on the morning side of the disk, which means that, for a uniform SO_2 mixing ratio, the detection would be easier on the morning side. We checked that a similar map is obtained if another weak CO_2 transition is used.

3. Search for SO_2

An examination of the TEXES integrated spectrum shows that no individual SO_2 transition is detected. Thus, we selected several transitions and co-added the spectrum at the positions of these transitions to improve the S/N. Nine lines were selected on the basis of their high S/N and the absence of telluric contamination. We note that the S/N expected from a given transition is not only a function of the line intensity, but also a function of the intrinsic noise level at this frequency. In the high-resolution, cross-dispersed mode of TEXES, the spectrum is indeed a combination of several echelon orders, which overlap. The S/N reaches a

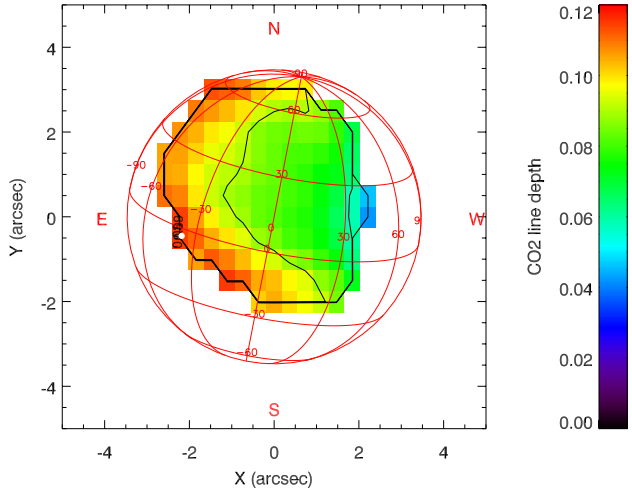

Fig. 4. The TEXES map of the line depth of the 1354.015 cm^{-1} CO_2 line. The radiances at the line center and in the continuum on each side of the line are each averaged over three frequency pixels. The spatial resolution is averaged over 1 arcsec in each dimension. The size of the Martian disk is 6 arcsec. The longitude of the central meridian is 140 E. Units are in arcsec in the celestial coordinates.

Table 1. Spectroscopic parameters of the nine SO_2 transitions used in the co-addition.

ν_0(cm^{-1})	I(cm^{-2} atm^{-1})	E(cm^{-1})
1351.1644	5.24×10^{20}	95.59
1352.0443	4.87×10^{20}	92.12
1353.5799	4.91×10^{20}	64.63
1353.7549	3.35×10^{20}	92.47
1353.9742	4.68×10^{20}	57.40
1353.9851	5.18×10^{20}	57.12
1356.6973	3.68×10^{20}	25.52
1356.742	3.44×10^{20}	30.00
1357.4798	3.03×10^{20}	24.67

maximum around the center of each order, so it varies along the spectrum, and the strongest transitions do not always correspond to the highest S/N. Table 1 lists the selected SO_2 transitions and their spectroscopic parameters. All lines show comparable intensities within a factor of two, and no weighting was applied in the summation.

Figure 5 shows the mean TEXES spectrum coadded in the vicinity of the nine selected transitions. A SO_2 signature, if present, would appear at the zero frequency, with a typical full width at half-maximum of 0.017 cm^{-1}, corresponding to the spectral resolution. To optimize the correction of the curvature effect, we used a third order polynomial, and checked that polynomials of higher degrees led to similar residuals. A comparison of the coadded disk-averaged TEXES spectrum with a third order polynomial (Fig. 5) shows that no line is present. Figure 6 shows the residual, binned over three spectral pixels, compared with synthetic models of SO_2 calculated with mixing ratios ranging from 0.3 to 2 ppb. The rms value of the residual is 0.0000675. We thus derive, from the TEXES disk-averaged spectrum, a 2σ upper limit of 0.3 ppb of SO_2, assuming a constant vertical mixing ratio. This result, however, is obtained assuming that our instrumental errors are combining using Gaussian statistics, which needs to be tested in the TEXES data analysis.

To search for possible local sources of SO_2 over the Martian disk, we mapped the line depth of the TEXES coadded spectrum

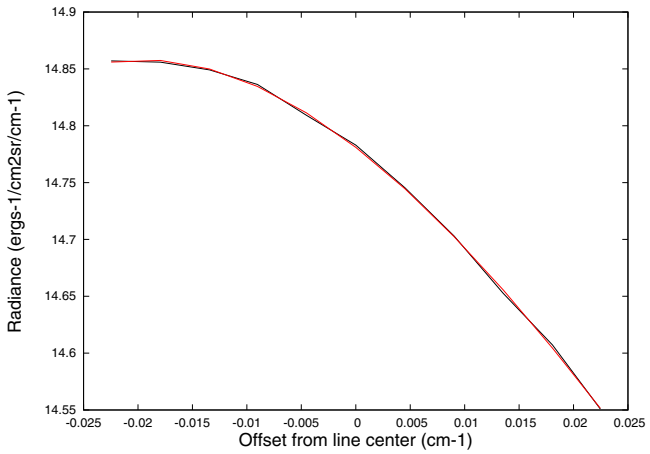

Fig. 5. Black line: the disk-averaged TEXES spectrum (same as Fig. 1) coadded in the vicinity of the nine SO_2 transitions listed in Table 1. All frequencies have been aligned on the zero frequency at the center of the figure. Red line: third order polynomial fit.

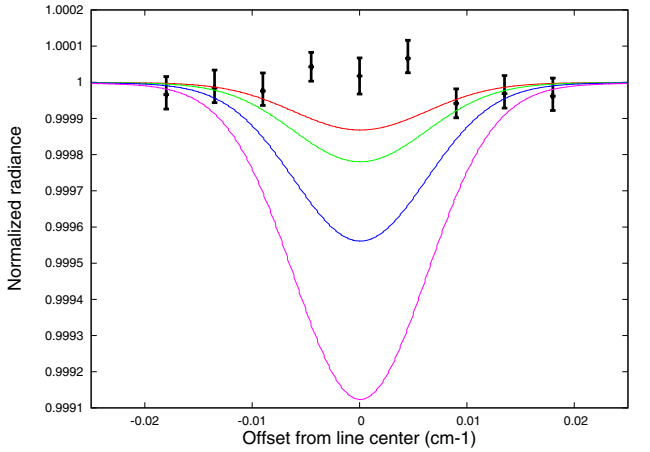

Fig. 6. Black points: the residual of the coadded disk-averaged TEXES spectrum, after subtraction of the third order polynomial (Fig. 5). Color lines: synthetic models. From top to bottom; [SO_2] = 0.3, 0.5, 1 and 2 ppb.

at the zero frequency. To estimate this line depth, we compared the radiance at the zero frequency (averaged over three spectral pixels) with the mean value of the continuum on each side of the line (also averaged over three pixels), and we divided the difference by the radiance at zero frequency. The result is shown in Fig. 7. It can be seen that the line depth value around the maximum radiance (Fig. 2) is slightly negative, which is due to the curvature of the TEXES co-added spectrum in this region (Fig. 5). It also appears that the variations over the disk are smaller than 0.001 over the whole disk. A comparison with synthetic models (Fig. 6) shows that the corresponding SO_2 mixing ratio is smaller than 2 ppb. The area observed by TEXES covers the longitude ranges 50 E–170 E for latitudes larger than 30 N, 100 E–170 E for latitudes between 0 and 30 N, and 110 E–170 E for latitudes between 15 S and 0. It can be seen that our upper limit of 2 ppb is slightly overestimated on the morning side of the map (longitude range 50 E–110 E): the synthetic SO_2 spectra (Fig. 6) are indeed calculated around the maximum radiance, where the CO_2 line depth is about 0.08 (Fig. 4). On the morning side, as shown in Fig. 4, the CO_2 line depth is larger by about

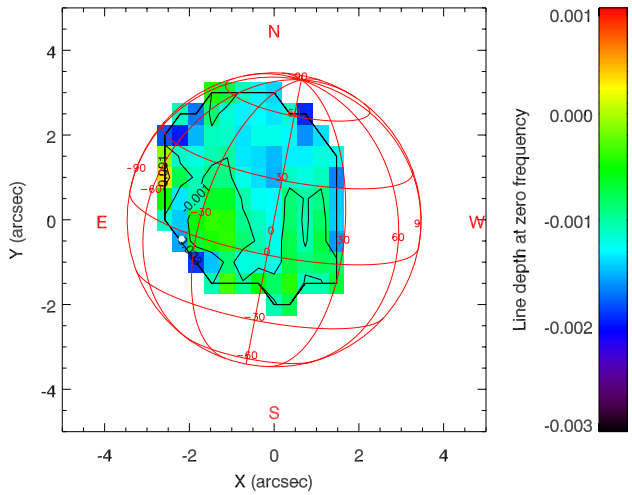

Fig. 7. The TEXES map of the line depth of the TEXES coadded spectrum around the zero-frequency (Fig. 5). The radiances at the center and in the continuum on each side of the line (2 pixels apart from the zero frequency) are each averaged over three frequency pixels. The spatial resolution is averaged over 1 arcsec in each dimension. The size of the Martian disk is 6 arcsec. The longitude of the central meridian is 140 E. Units are in arcsec in the celestial coordinates.

30%. The corresponding upper SO_2 limit in this region is thus about 1.5 ppb.

4. Discussion

From our analysis, we have derived a 2σ SO_2 upper limit of 0.3 ppb in the region of maximum radiance (centered at 30 N, 140 E). This value is three times smaller than the previous upper limit derived by Krasnopolsky (2005), who also used TEXES data obtained in June 2003. The improvement shown in the present study is probably due to the choice of a different spectral range and a longer integration time.

Using the mapping capability of TEXES, we conclude that, at 1 arcsec resolution (which corresponds to a field of view of about 1000 km), no SO_2 source stronger than 2 ppb is present in the northern hemisphere, in the longitude range mentioned above. This area covers, in particular, the volcanic region of Elysium where some weak outgassing activity, if present on Mars, might have been detected. This region also covers the site of the Gusev crater where sulfates were detected by the Spirit rover, as well as high northern latitudes where gypsum was detected (80 N). We note that the longitude range of the gypsum signature (220 E–240 E) is not covered by the TEXES observations. However, if some episodic outgassing were taking place over the gypsum region, the gaseous SO_2 emitted in the atmosphere very close to the pole would quickly spread in longitude in less than a week. We can thus conclude that no SO_2 outgassing occurred over the gypsum region at the time of the TEXES observations (October 2009).

The absence of localized SO_2 sources over the Martian disk is consistent with the expectations. The SO_2 lifetime is indeed longer than the global mixing timescale of the Martian atmosphere (Krasnopolsky 2005; Wong et al. 2003, 2005). In this case, the spatial distribution of a non-condensible species is expected to be nearly uniform around equinox, as modeled in the case of CO (Forget et al. 2006) and CH_4 (Lefèvre & Forget 2009). Our SO_2 upper limit of 0.3 ppb is thus likely to apply to the whole disk. In addition, there is no reason to expect a

correlation between the presence of gaseous SO_2, if it exists, and the location of sulfates: these sulfates are indeed tracers of past liquid water, while gaseous SO_2, if outgassed from a volcanic source, is rapidly distributed over the disk.

Finally, as pointed out by Krasnopolsky (2005), the non-detection of SO_2 seepage at the Martian surface has some implications for the possible origin of methane on Mars, if its detection is confirmed. In the terrestrial volcanoes, the SO_2 to CH_4 ratio typically ranges between 10^2 and 10^4. To first order, a comparable volcanic composition can be expected on Mars. If localized and transient methane sources are indeed present at a level of more than 10 ppb, then a volcanic origin for these sources is unlikely.

Future observations will benefit from the use of the EXES instrument aboard the SOFIA airborne observatory. This echelon cross-echelle spectrograph, very similar to TEXES, will operate in the 4.5–28.3 μm range with a spectral resolving power as high as 10^5 (Richter et al. 2010). Observing at an altitude of about 14 km will allow us to drastically reduce the terrestrial contamination by water vapor and methane, and permit a more sensitive and simultaneous search for SO_2 and CH_4 on Mars.

Acknowledgements. T.E., T.K.G., M.J.R., and J.H.L. were Visiting Astronomers at the Infrared Telescope Facility, which is operated by the University of Hawaii under Cooperative Agreement No. NNX-08AE38A with the National Aeronautics and Space Administration, Science Mission Directorate, Planetary Astronomy Program. We thank the IRTF staff for the support of TEXES observations. Observations with TEXES were supported by N.S.F. Grants AST-0607312 for J.H.L. and AST-0708074 for M.J.R. T.K.G. acknowledges support by NASA Grant NNX08AW33G S03 for data reduction. T.E. and B.B. acknowledge support from CNRS, and T.F. aknowledges support from UPMC.

References

Christensen, P. R., Wyatt, M. B., Glotch, T. D., et al. 2004, Science, 306, 1733
Encrenaz, T., Bézard, B., Greathouse, T. K., et al. 2004, Icarus, 170, 424
Encrenaz, T., Bézard, B., Owen, T., et al. 2005, Icarus, 179, 43
Encrenaz, T., Greathouse, T. K., Richter, M. J., et al. 2008, Icarus, 195, 547
Encrenaz, T., Greathouse, T. K., Bézard, B., et al. 2010, A&A, 520, A33
Encrenaz, T., Greathouse, T. K., Lefèvre, F., & Atreya, S. K. 2011, Plan. Space Sci., submitted
Forget, F., Hourdin, F., Fournier, R., et al. 1999, J. Geophys. Res., 104, 24155
Forget, F., Montabone, L, & Lebonnois, S. 2006, Second International Workshop on Mars Atmosphere Modelling and Observations, Granada, Feb. 27–Mar. 3, Abstract 4.2.2
Formisano, V., Atreya, S., Encrenaz, T., Ignatiev, N., & Giuranna, M. 2004, Science, 306, 1758
Jacquinet-Husson, N., Scott, N., Chedin, A., et al. 2008, J. Quant. Spectr. Rad. Transfer, 109, 1043
Johnson, J. R., Bell, J. F., Cloutis, E., et al. 2007, Geophys. Res. Lett., 34, L13202
Krasnopolsky, V. 2005, Icarus, 178, 487
Lacy, J. H., Richter, M. J., Greathouse, T. K., et al. 2002, Pub. Astron. Soc. Pacific, 114, 153
Langevin, Y., Poulet, F., Bibring, J.-P., & Gondet, B. 2005, Science, 307, 1584
Lefèvre, F., & Forget, F. 2009, Nature, 460, 720
Mumma, M. J., Villanueva, G. L., Novak, R. E., et al. 2009, Science, 323, 1041
Nakagawa, H., Kasaba, Y., Maezawa, H., et al. 2009, Plan. Space Sci., 57, 2123
Neukum, G., Jaumann, R., Hoffmann, H., et al. 2004, Nature, 432, 971
Pollack, J. B., Roush, T., Witteborn, F., et al. 1991, J. Geophys. Res., 95, 14595
Richter, M. J., Ennico, K. A., McKelvey, M. E., & Seifahrt, A. 2010, Proc. SPIE, 7735, 77356Q
Rieder, R., Gellert, R., Anderson, R. C., et al. 2004, Science, 306, 1746
Roush, T., Pollack, J. B., Stoker, C., et al. 1989, LPSC Abstract, 80
Squyres, S. W., Grotzinger, J. P., Arvidson, R. E., et al. 2004, Science, 306, 1709
Toulmin, P., Rose, H. J., Christian, R. P., et al. 1977, J. Geophys. Res., 82, 4625
Wong, A. S., Atreya, S. K., & Encrenaz, T. 2003, J. Geophys. Res., 108 (E4), 5026; Correction: J. Geophys. Res., 110, E10002